Indian Journal of Radio & Space Physics
Vol 44, September 2015, pp 113-121

Investigations of slow and fast coronal mass ejections and their associated activities in Solar cycle 24

M Bendict Lawrance[1,$,*], A Shanmugaraju[2,#] & S Prasanna Subramanian[3]

[1]Sethu Institute of Technology, Kariapatti, Virudhunagar Dist 626 115, India

[2]Arul Anandar College, Karumathur 625 514, Madurai Dist, India

[3]M K University College, Aundipatti, Theni Dist 625 531, India

E-mail: [$]Lorentz.ben@gmail.com; [#]ashanmugaraju@gmail.com

Received 1 April 2015; revised received and accepted 6 October 2015

The present papers compares the properties of slow and fast coronal mass ejections (CMEs) associated with intensive flare (>M5.0 X-ray class) during 2008-2013 in solar cycle 24. The CMEs are separated into two groups based on speed: Group I containing 31 CME events with speed below 900 km s^{-1} and Group II containing 27 CME events with speed above 900 km s^{-1}. The mean CME speeds of Groups I and II are found to be 558 and 1629 km s^{-1}, respectively and the mean CME width of the Group II is slightly higher than Group I. The CMEs of Group II are highly decelerated than the CMEs of Group I. It is found that the rise time and duration of intensive flares of Group II is slightly greater than those of Group I. While 60% of Group I events are located on the southern hemisphere, 85% of Group II events are located on the northern hemisphere. Further, the number of halos, DH type IIs, Solar energetic particle (SEP) events associated with Group II are 2, 3 and 6 times, respectively that of Group I. Utilizing the density models of suitably connecting the corona and interplanetary medium, the shock formation height of DH type radio bursts are found to be in the height range 2-6 $R_\odot$ and the maximum estimated distance of shock are found to be in the height range 16-215 $R_\odot$. The mean shock speed of Group I and Group II events (599 and 1359 km s^{-1}, respectively) are in agreement with the CME speed. On comparison of slow and fast events, the faster events are found to be mostly decelerated, mostly associated with stronger storms, more number of DH type II bursts and SEPs.

Keywords: Solar cycle, Solar flares, Coronal mass ejections, Radio burst, Solar energetic particle

PACS Nos: *96.60.ph*; *96.60.qe*; *96.60.tg*

1 Introduction

Coronal mass ejections (CMEs) are large scale magnetized plasma structure originated from the Sun and ejected into the interplanetary medium through solar corona. They are important source for various activities, like geomagnetic storms and solar energetic particle (SEP) emission. CMEs have been observed using coronagraphs in Solar and Heliospheric Observatory (SOHO) / Large Angle Solar Coronagraph (LASCO) and Solar Terrestrial Relations Observatory (STEREO) missions[1,2]. As it is known, CMEs also have been observed using coronagraphs in Orbiting Solar Observatory-7 (OSO-7), Skylab, P78-1, Solar Maximum Mission (SMM), and Yohkoh[3]; solar flares are also observed in H-alpha wavelength by spacecraft. They are classified as A, B, C, M and X class according to the peak flux of X-ray intensity (10^{-8} to 10^{-4} watts m^{-2}) as measured by GOES spacecraft. Many of the strong flare-CME associated events are related with major SEP emission above 10 particle flux unit (pfu) (Ref. 4). Generally, CME speed lies between 200 and 2000 km s^{-1}, CMEs below 400 km s^{-1} speed are accelerated and CMEs above 400 km s^{-1} are decelerated by solar wind interaction[5].

Chandra *et al.* [6] compared the properties of CMEs associated with SEP events and type II bursts in the rising phases of Solar cycle (SC) 23 and 24. They grouped the events according to SEP intensity as weak (intensity < 1 pfu), minor (1 pfu < intensity < 10 pfu) and major (intensity => 10 pfu). They found that most of the major SEP events are associated with halo CMEs originated close to the sun center and western hemisphere. Also, the fraction of halo CMEs in SC 24 is larger than the SC 23 and for major SEP events, the average CME speeds are higher in comparison to the minor and weak events.

According to Yashiro & Gopalswamy[7], the flare-CME association rate increases with peak flux, fluence and duration of flare. In an another study, the

CMEs and their associated activities for the period 1997-2006 were analyzed by Gopalswamy *et al.*[8] and they reported that CMEs associated with type II bursts events having emission components at all wavelengths (metric to kilometric) produce large SEP events. Hence, the study of strong flares and their associated activities are important. A majority of CMEs producing DH type II bursts have mean speed around 900 km s^{-1} and they were found to be associated with SEP events[9-11]. The aim of the present work is to compare the properties of slow (V < 900 km s^{-1}) and fast CMEs (V > 900 km s^{-1}) associated with intensive flares; and to study their associated effects, such as DH type II radio bursts, SEP events and geomagnetic storms.

2 Data selection

The events, observed during December 2008 - December 2013 in solar cycle 24, were classified into two groups based on the CME speed (V < 900 km s^{-1} as Group I and V > 900 km s^{-1} as Group II). Since 900 km s^{-1} indicates the average Alfvenic velocity[10], it was chosen as a critical velocity. These events were associated with intensive X-ray flares of flare-class above M5.0. All the X-ray flare data were obtained from the online data catalog maintained by Solar Geophysical Data Centre (http://www.ngdc.noaa.gov/stp/space-weather/solar-data/solar-features/solar-flares/x-rays/goes/). The CME data were taken from the online CME catalog http://cdaw.gsfc.nasa.gov/CME (Ref. 11). The first detection time of a CME in LASCO-C2 has to be within an hour after the flare onset and their source locations were also checked. One-hour is chosen as time window because most of the CMEs reach the LASCO C2 field of view within one hour from the flare onset[12]. The data of DH type II radio burst were taken from the list available in http://cdaw.gsfc.nasa.gov/CME_list/radio/waves_type2.html. The Solar Energetic Particle (SEP) proton data at energy >10 Mev in particle flux unit (pfu) was considered from the website http://umbra.nascom.org [since these major SEPs are believed to be associated with the earth directed CMEs[5]].

Using the above selection criteria, 58 events were selected out of 67 flares of >M5.0 in the solar cycle 24. Nine events were excluded due to unclear flare location or non-CME association. The events were classified according to CME speed, as Group I containing 31 slow speed CME events (<900 km s^{-1}) and Group II containing 27 high speed CME events (>900 km s^{-1}). Flare, CME and their associated activities of Group I and II are listed in Tables 1 and 2, respectively. All the CME data (date, year, time of first detection in LASCO, speed, acceleration, CPA and width); the flare data [location, onset time, rise time (Fr), duration (Fd) and GOES X-ray flare-class]; the SEP intensity (in pfu) and presence of type II radio burst in DH (decameter-hectometric) range and the Dst index are listed in these tables. A set of 12 events is found to be associated with proton emission of particle flux >10 pfu. These events are notable events listed in NOAA space weather alerts (www.solarcycle24.com).

3 Results and Discussion

3.1 Properties of solar flares

Figure 1 shows the flare locations associated with slow (Group I) and fast CME (Group II) events. The distribution of solar flare location of Group I events shows that 61% (19 out of 31) events are located in

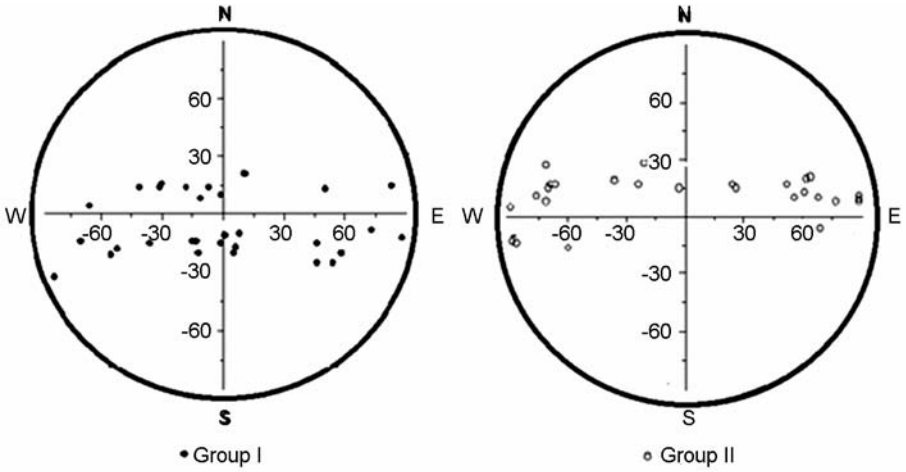

Fig. 1 — Distribution of flare locations: (left) Group I; (right) Group II

the southern hemisphere of the sun. On the other hand, the right panel in Fig. 2 shows 85% (23 out of 27) Group II events are located in the northern hemisphere. All the events are located between ±32 degrees in latitude from the solar equator. This shows that the intensive flare associated fast halo CMEs/SEPs are active in the northern hemisphere of the sun. Hence, the North-West quadrant is found to be mostly occupied by Group II events. This is consistent with Chandra *et al.*[5] that the SEPs source regions are mostly in the northern hemisphere during the rising phase of solar cycle 24.

The distribution of number of events in flare classes of M5.0 - M10.0, X0.0 - X5.0 and X5.1 – X10.0 are shown in Fig. 2. The left panel shows the distribution of X-ray flare class of Group I events. More number of events (65%, 20 out of 31) are distributed between the flare class of M5.0-M10.0. The right panel shows the distribution of X-ray flare class of Group II events. In contrast to Group I, nearly equal number of events is distributed between the M and X-class for Group II. Rise time and duration of the flares are estimated and their distributions are shown in Fig. 3. It is clearly evident from this figure that the Group II flares are more than two times longer than Group I. The mean flare rise time of Group I and Group II events are found to be 14 and 30 minutes, respectively. Similarly, the mean flare duration of Group I and Group II events are found to be 23 and 51 minutes, respectively. The longer duration of flare refers the prolonged energy input to the initial acceleration of CMEs[13] and so, the high speed of CMEs. For example, Annalakshmi & Umapathy[14] studied the CME properties of short and long duration flares in which they found that the CMEs associated with long duration flares have greater mean speed. From the values in Tables 1 and 2, 70% of the Group II events (19 out of 27) are found

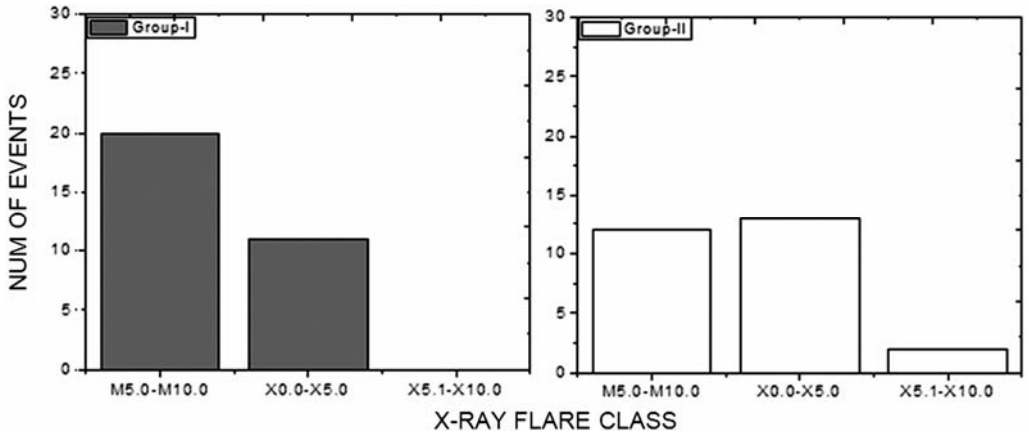

Fig. 2 — Distribution of number of intensive X-ray flares: (left panel) Group I; (right panel) Group II.

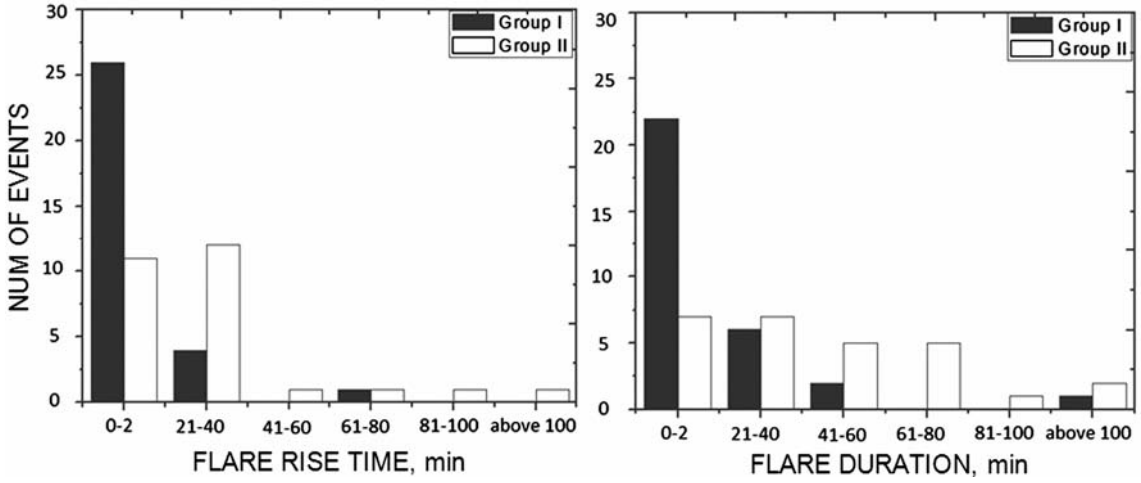

Fig. 3 — Distribution of flare: rise time (left); and duration (right) for Group I and Group II

Table 1 — List of slower Group I CME events and their associated activities in solar cycle 24

S No	CME							Flare					SEP	Dst
	DD-Mon	Year	Time, hh:mm UT	Speed, km s^{-1}	Accelaration, m s^{-2}	CPA, deg	Width, deg	Location	Time, hh:mm UT	Fr, min	Fd, min	Flare Class	SEP, pfu	Index, nT
1	07-Feb	2010	03:54	421	0.5	Halo	360	N21E11	02:20	14	19	M6.4	-	-7[a]
2	12-Feb	2010	13:42	509	-18.3*	Halo	360	N21E10	11:19	7	9	M8.3	-	-59[b]
3	06-Nov	2010	16:12	178	5.3*	109	33	S20E58	15:27	9	17	M5.4	-	-
4	13-Feb	2011	18:36	373	24.4*	359	276	S20E05	17:28	10	19	M6.6	- /Dh	-
5	15-Feb	2011	02:24	669	-18.3	Halo	360	S20W12	01:44	12	22	X2.2	- /Dh	-32[a]
6	18-Feb	2011	12:12	350	93.8*	281	89	S21W55	09:55	16	20	M6.6	-	-
7	09-Mar	2011	23:05	332	-23*	356	155	N08W11	23:13	10	16	X1.5	-	-
8	03-Aug	2011	14:00	610	-12.2*	Halo	360	N16W30	13:17	31	53	M6.0	-	-115[b]
9	06-Sep	2011	02:24	782	105.6*	Halo	360	N14W07	01:35	15	30	M5.3	- /Dh	-
10	06-Sep	2011	23:05	575	1.1*	Halo	360	N14W18	22:12	8	12	X2.1	- /Dh	-75[a]
11	07-Sep	2011	23:05	792	-3.1*	299	167	N14W31	22:32	6	12	X1.8	-	-
12	08-Sep	2011	16:36	214	16.9*	317	37	N14W41	15:32	14	20	M6.7	-	-
13	25-Sep	2011	05:12	788	-22.5*	98	193	N13E50	04:31	19	34	M7.4	- /Dh	-
14	02-Jul	2012	11:24	313	-3.2	174	125	S17E06	10:43	9	14	M5.6	-	-
15	05-Jul	2012	13:24	741	1.9	219	98	S18W52	11:39	5	10	M6.1	-	-
16	12-Jul	2012	16:48	885	195.6*	Halo	360	S15W01	15:37	72	113	X1.4	96/ Dh	-127[a]
17	28-Jul	2012	21:12	420	-6.8	Halo	360	S25E54	20:44	12	20	M6.1	-	-
18	20-Oct	2012	18:36	330	-4.2*	76	130	S12E88	18:05	9	14	M9.0	-	-
19	13-Nov	2012	02:24	851	-10.9	119	141	S25E46	01:58	6	8	M6.0	-	-
20	11-Apr	2013	07:24	861	-8.1	Halo	360	N10W01	06:55	21	34	M6.5	114/Dh	-6[a]
21	03-May	2013	18:05	858	-8	86	274	N15E83	17:24	8	17	M5.7	-	-
22	07-Jun	2013	23:12	770	-2.2	204	150	S32W83	17:24	8	17	M5.7	-	-
23	24-Oct	2013	01:25	399	-17	Halo	360	S10E08	00:21	9	14	M9.7	-	-
24	25-Oct	2013	08:12	587	-13.7	Halo	360	S08E73	07:53	8	16	X1.7	-	-
25	28-Oct	2013	02:24	695	-12.1	Halo	360	N04W66	01:41	22	31	X1.0	-	-
26	01-Nov	2013	20:24	268	3.7	179	42	S11E01	19:46	7	12	M6.3	-	-
27	05-Nov	2013	22:36	562	-5.8	160	195	S15E46	22:07	5	8	X3.3	-	-
28	08-Nov	2013	03:24	497	11.7	Halo	360	S14W15	04:20	6	9	X1.1	-	-
29	10-Nov	2013	05:36	682	-41.8	220	262	S14W13	05:08	6	10	X1.1	-	-
30	19-Nov	2013	10:36	740	-2	Halo	360	S14W70	10:14	12	20	X1.0	- / Dh	-
31	31-Dec	2013	22:36	271	2.9	237	87	S15W36	21:45	13	35	M6.4	-	-

to be decelerated in contrast to 58% of Group I events (18 out of 31). This result is consistent with the result of Yashiro *et al.* [3], Manoharan *et al.*[15], Manoharan[5] and also Annalakshmi & Umapathy[14] in which they reported that the faster CMEs (> 900 km s^{-1}) are mostly decelerated.

3.2 Properties of Coronal Mass Ejection

The CME speed for Group I and Group II events are different in the ranges 178 - 861 km s^{-1} and 950 - 2684 km s^{-1}, respectively. Figure 4 shows the distribution of CME speed. The mean CME speed for Group I and Group II events are found to be 557 and 1629 km s^{-1}, respectively. Figure 5 shows the distribution of CME width. The CME width of Group I events lie in the range 33-360 degrees, whereas the width of Group II CMEs lie mostly around 300-360degrees.

Table 3 shows the solar activity association rate (flares, CMEs, DH Type IIs and SEPs). The associated activities such as DH type II and SEP are found to be very less in Group I as compared to Group II. The reason is mainly the speed of the CMEs. The slow speed events in Group I most probably do not able to drive a strong shock and hence not able to produce DH type IIs and also not able to accelerate SEPs[10].

Table 2 — List of faster Group II CME events and their associated activities in solar cycle 24

S No	CME							Flare					SEP	Dst
	DD-Mon	Year	Time, hh:mm UT	Speed, km s^{-1}	Accelaration, m s^{-2}	CPA, deg	Width, deg	Location	Time, hh:mm UT	Fr, min	Fd, min	Flare Class	SEP, pfu	Index, nT
1	04-Aug	2011	04:12	1315	-41.1	Halo	360	N19W36	03:41	16	23	M9.3	96/Dh	-115[a]
2	09-Aug	2011	08:12	1610	-40.6	Halo	360	N17W69	07:41	17	20	X6.9	26/Dh	-
3	22-Sep	2011	10:48	1905	-68.3	Halo	360	N09E89	10:29	32	75	X1.4	35/Dh	-5[b]
4	24-Sep	2011	09:48	1936	-25*	92	145	N13E61	09:21	19	27	X1.9	-	-
5	24-Sep	2011	12:48	1915	79.6	Halo	360	N10E56	12:33	37	97	M7.1	-/Dh	-118[a]
6	03-Nov	2011	23:30	991	-40.5	Halo	360	N21E64	20:16	11	16	X1.9	-	-
7	23-Jan	2012	04:00	2175	28	Halo	360	N28W21	03:38	21	56	M8.7	6310/Dh	-73[b]
8	27-Jan	2012	18:27	2508	165.9	Halo	360	N27W71	17:37	60	79	X1.7	796/Dh	-
9	05-Mar	2012	04:00	1531	-24.6	Halo	360	N17E52	02:30	99	133	X1.1	-/Dh	-72[b]
10	07-Mar	2012	01:30	1825	-160	Halo	360	N15E26	01:05	9	18	X1.3	-	-
11	07-Mar	2012	00:24	2684	-88.2	Halo	360	N17E24	00:02	22	38	X5.4	6530/Dh	-131[a]
12	09-Mar	2012	04:26	950	-13.5*	Halo	360	N15W03	03:22	31	56	M6.3	-/Dh	-29[b]
13	10-Mar	2012	18:12	1379	24.1	Halo	360	N17W24	17:15	29	75	M8.4	-/Dh	-50[b]
14	13-Mar	2012	17:36	1884	45.6	Halo	360	N17W66	17:12	29	73	M7.9	469/Dh	-74[a]
15	17-May	2012	01:48	1582	-51.8	Halo	360	N11W76	01:25	22	49	M5.1	255/Dh	-
16	06-Jul	2012	23:24	1828	-56.1	Halo	360	S13W59	23:01	7	13	X1.1	25/Dh	-
17	08-Jul	2012	16:54	1495	-85.3	219	157	S14W86	16:23	9	19	M6.9	-/Dh	-
18	19-Jul	2012	05:24	1631	-8	Halo	360	S13W88	04:17	101	159	M7.7	-/Dh	-
19	18-Aug	2012	00:48	986	12.5	62	145	N20E62	00:24	38	43	M5.5	-	-
20	13-May	2013	02:00	1270	15.9	Halo	360	N11E89	01:53	24	39	X1.7	-/Dh	-
21	13-May	2013	16:07	1850	-76.6	Halo	360	N08E89	15:48	17	28	X2.8	-/Dh	-
22	14-May	2013	01:25	2625	-51	Halo	360	N08E77	00:00	71	80	X3.2	-/Dh	-
23	15-May	2013	01:48	1366	-52.1	Halo	360	N10E68	01:25	23	33	X1.2	41/Dh	-55[b]
24	22-May	2013	13:35	1466	-13.2	Halo	360	N15W70	13:08	24	60	M5.0	1660/Dh	-48[a]
25	25-Oct	2013	15:12	1081	-25.2	Halo	360	S06E69	14:51	13	21	X2.1	-/Dh	-
26	28-Oct	2013	04:48	1201	-45.2	315	156	N08W71	04:32	9	14	M5.1	-/Dh	-
27	29-Oct	2013	22:00	1001	-29.7	Halo	360	N05W89	21:42	12	19	X2.3	-	-

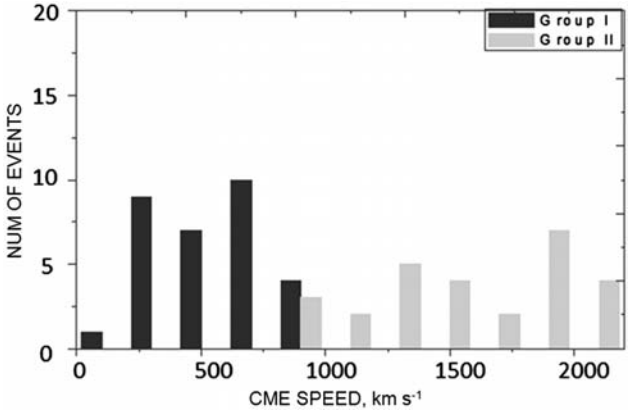

Fig. 4 — Distribution of CME speed for Group I and Group II

Table 3 — Number of intensive flares and their associated events in cycles 23 and 24

Activity	Number of events	
	Group I (31)	Group II (27)
M5-M10 class flare	20 (65%)	12 (44%)
X1-X5 class flare	11 (36%)	13 (48%)
X5-X10 class flare	0 (0%)	2 (7%)
Geomagnetic storms	7 (23%)	11 (41%)
Halo CMEs	14 (45%)	23 (85%)
DH Type II bursts	8 (26%)	22 (81%)
SEP events	2 (7%)	11 (41%)

3.3 Properties of interplanetary type II radio bursts

As seen in Table 3, only 26% of CMEs in Group I have produced DH type II bursts in contrast to 81% of Group II events. Table 4 shows the properties of DH type II associated with CME events, viz. CME data (date, year, time of first detection in LASCO, speed); and radio burst data (drift rate, start distance, end distance, shock speed). The starting frequency of most of DH type II events varies between 16 and 1.5 MHz. The starting and ending frequencies indicate the height at which the plasma radio emission from the

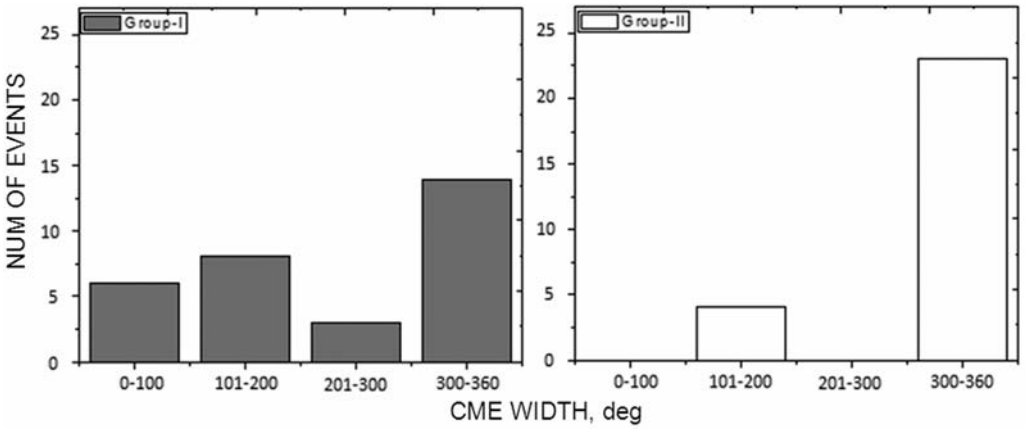

Fig. 5 — Distribution of CME width for: (left) Group I; (right) Group II

Table 4 — Properties of DH Type II Radio bursts corresponding to the Group I and II CMEs

S No	CME				Type II Radio burst			
	DD-Mon	Year	Time, hh:mm UT	Speed, km s^{-1}	Drift rate, KHz s^{-1}	Start distance, $R_\odot$	Maximum distance, $R_\odot$	Shock speed, km s^{-1}
	Group I							
1	13-Feb	2011	18:36	373	13.3	2.4	3	696
2	15-Feb	2011	02:24	669	0.9	2.4	26.1	948
3	06-Sep	2011	02:24	782	0.18	2.8	51.8	437
4	06-Sep	2011	23:05	575	0.26	2.4	69	750
5	25-Sep	2011	05:12	788	4.44	2.4	3	232
6	12-Jul	2012	16:48	885	0.24	2.8	41.5	460
7	11-Apr	2013	07:24	861	0.35	2.7	30	671
8	19-Nov	2013	10:36	740	0.4	2.8	102	1979
	Group II							
1	04-Aug	2011	04:12	1315	0.1	2.9	170	879
2	09-Aug	2011	08:12	1610	13.3	2.4	4.1	1315
3	22-Sep	2011	10:48	1905	0.3	2.8	150	2203
4	24-Sep	2011	12:48	1915	0.44	2.4	34.6	627
5	23-Jan	2012	04:00	2175	0.13	2.4	215	1174
6	27-Jan	2012	18:27	2508	0.43	2.4	69	1256
7	05-Mar	2012	04:00	1531	0.52	2.4	26.1	550
8	07-Mar	2012	00:24	2684	0.11	2.4	250	1141
9	09-Mar	2012	04:26	950	1.88	2.8	10.9	817
10	10-Mar	2012	18:12	1379	0.21	2.8	250	2571
11	13-Mar	2012	17:36	1884	0.68	2.4	51.8	1488
12	17-May	2012	01:48	1582	0.93	2.4	34.6	1334
13	06-Jul	2012	23:24	1828	0.97	2.4	34.6	1383
14	08-Jul	2012	16:54	1495	0.2	2.4	34.6	1149
15	19-Jul	2012	05:24	1631	1.47	4.5	17.5	3016
16	13-May	2013	02:00	1270	5.83	2.4	6.2	1102
17	13-May	2013	16:07	1850	1.5	2.4	34.6	2075
18	14-May	2013	01:25	2625	3.23	2.4	14.9	1834
19	15-May	2013	01:48	1366	0.77	10.1	41.5	2023
20	22-May	2013	13:35	1466	0.11	2.4	69	315
21	25-Oct	2013	15:12	1081	0.59	2.4	51.8	1290
22	28-Oct	2013	04:48	1201	0.53	2.4	51.8	1321

shocks becomes visible[16,17]. The type II's starting height was estimated using Hybrid electron density model[18], and the type II ending height was estimated using 2-fold Leblanc electron density model[19]. The hybrid model is valid for the distance > 1.2 $R_\odot$. The distance of shock in Group I events lies in the height range 3-42 $R_\odot$. In Group II, the shock distance lies between 4 and 250 $R_\odot$. It means that the Group II shocks can reach longer distance than Group I. Pohjolainen *et al.*[20] studied about the origin of wide band IP type II bursts and found that the both CME-solar wind interaction and synchrotron mechanism are the important cause of production of IP type II bursts. They reported the association of wide band IP type II burst with SEP emission. In the present study, all the SEP events in both groups are found to be associated with DH type II bursts. Chandra *et al.*[5] reported that the average CME speeds of major SEPs are higher in comparison to the minor and weak events in solar cycle 24. Likewise, in the present study, the Group II faster events are found to be mostly associated with major SEPs. The shock speed was estimated using the following relation:

$$V_{shock} = \Delta H/\Delta t = (H_{IIstart} - H_{IIend}) / (T_{IIstart} - T_{IIend})$$

where, $H_{IIstart}$ and H_{IIend}, are the type II starting and ending heights determined using the density models; $T_{IIstart}$ and T_{IIend}, are the starting and ending times of Type II noted from the observations. The mean shock speed of DH type II bursts in Group I is 599 km s^{-1} and that of Group II is 1359 km s^{-1}. In the IP medium, the shock/CME acceleration mainly depends on solar wind speed, density, CME initial speed and the ejection of any pre-CMEs from the same or nearby active region. The heights of radio emissions corresponding to the starting and ending frequencies of all DH type IIs of both groups are shown in Fig. 6, where most of the DH type II emission started between 2 and 10 $R_\odot$ in both groups. The plasma emission frequencies between 16 and 2 MHz occur in that distance range[19]. In certain events, the starting frequency 16 MHz may be the continuum frequency emission from metric band to DH band. Gopalswamy *et al.*[11] found the shock formation (using wave diameter and leading edge methods) heights substantially below 1.5 $R_\odot$ for CMEs associated with metric type II bursts and mentioned that few cases was close to 2 $R_\odot$. But, in the present study, DH type II bursts have been selected and the shock formation is, thus, greater than 2 $R_\odot$. The shock producing CMEs are able to accelerate particles and produce SEP events.

The mean ending frequency of Group II (~ 0.5 MHz) events is comparably higher than that of Group I (~ 0.2 MHz) events. It is due to the speed that the driftness in the faster CMEs extends in a more precise way. It suggests that the shocks associated with slow CMEs with lesser kinetic energy in Group I may become weaker[13] at a faster rate. On the other hand, the lower ending frequencies of DH type II radio emission of Group I and II events suggest that their shocks are stronger up to a very long distance in the IP medium.

3.4 Geomagnetic storms

The Dst index were noted from Richardson/Cane list (http://www.srl.caltech.edu/ACE/ASC/DATA/level3/icmetable2.htm), which are marked as 'a' in the last column of Tables 1 and 2. Also, storms data were collected separately from http://wdc.kugi.

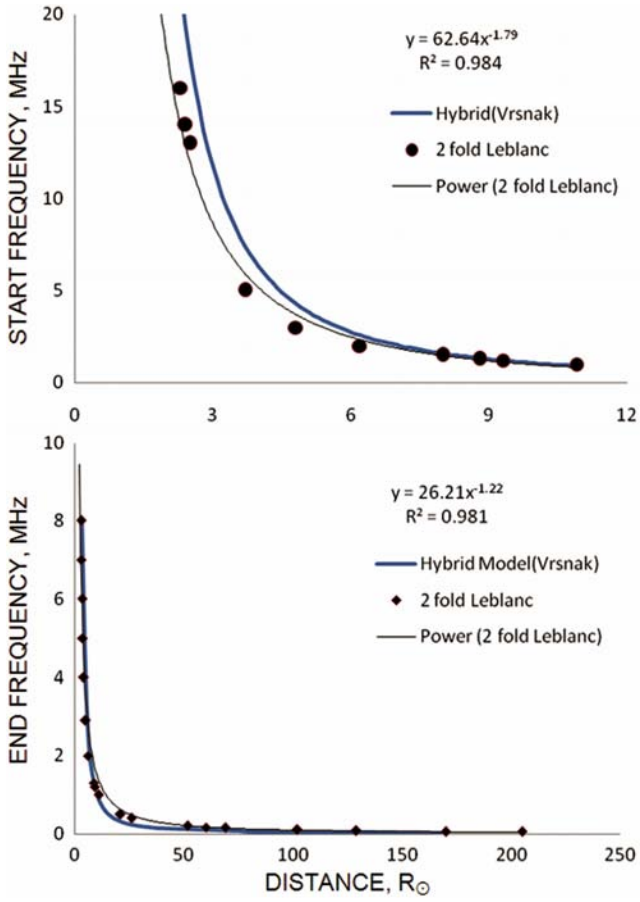

Fig. 6 — (Top): Starting frequency versus distance derived from electron density models [Hybrid model and Leblanc model] in the DH frequency range; (Bottom): Ending frequency versus distance

kyoto-u.ac.jp/Dst_provisional/index.html during the ICME/IP shock arrival time taken from http://umtof.umd.edu/pm/FIGS.HTML for certain events and they are marked as 'b' in the last column of Tables 1 and 2. It is found that 7 events in Group I and 11 events in Group II produced geo-magnetic storms. The mean Dst index of the Group I events is -55 nT and the Group II events is -70 nT. The fast CMEs have produced slightly stronger storm (greater negative Dst) than the slow CMEs. It is in agreement with the results of Srivatsava & Venkatakrishnan[21].

4 Conclusions

The properties of slower and faster CMEs associated with strong X-ray flares of class > M5.0 in solar cycle 24 are analyzed. Also, their effects/ associated activities such as, X-ray flares, DH type II radio bursts, SEPs and geomagnetic storms are compared. The following results are emerged from this study:

(i) The mean CME speed of Groups I and II are found to be 558 and 1629 km s^{-1}. The mean CME width of Group II is slightly higher than the Group I CMEs. The CMEs of Group II are highly decelerated than the CMEs of Group I.

(ii) The rise time and duration of intensive flares of Group II are slightly greater than those of Group I.

(iii) The shock formation height of DH type radio bursts is found to be in the height range 2-10 $R_\odot$. This result is in agreement with the result of Gopalswamy *et al.*[11] that they estimated the shock height of metric type II burst as 1.5 – 2 $R_\odot$ but in the present study the DH type II formation exceeds 2 $R_\odot$.

(iv) The maximum distance reached by the shocks of Group II are found to be little longer in the height range 16 - 215 $R_\odot$ than Group I events.

(v) The mean shock speed of Group I and Group II events are estimated to be 599 and 1359 km s^{-1}, respectively which is similar to those of CME speeds.

(vi) The Group II faster events are found to be mostly associated with major SEPs, which is in consistent with Chandra *et al.*[5].

(vii) The mean Dst of Group I and Group II events are found to be -55 and -70 nT, respectively.

The above results indicate that the faster events are more associated with stronger storms, more number of DH type II bursts and SEPs.

Acknowledgement

The authors gratefully acknowledge the data support provided by various online data centers of NOAA and NASA. They would like to thank the Wind/WAVES team for providing the Type-II catalogs. The CME catalog used is provided by the Center for Solar Physics and Space Weather, The Catholic University of America in cooperation with the Naval Research Laboratory and NASA. They also thank Dr P K Manoharan, TIFR for constructive discussions and support. One of the authors (AS) acknowledges the major research grant No. 42–845/2013 (SR) from University Grants Commission, Govt of India. They also thank the referees for useful comments to improve the quality of this manuscript.

References

1 Brueckner G E, Howard R A, Koomen M J, Korendyke C M, Michels D J, Moses J D, Socker D G, Dere K P, Lamy P L, Llebaria A, Bout M V, Schwenn R, Simnett G M, Bedford D K & Eyles C J, The large angle spectroscopic coronagraph (LASCO), *Sol Phys (Netherlands)*, 162 (1995) pp 357-402.

2 Kaiser M L, Kucera T A, Davila J M, St Cyr O C, Guhathakurta M & Christian E, The STEREO Mission: An introduction, *Space Sci Rev (Netherlands)*, 136 (1) (2008) pp 5-16.

3 Yashiro S, Gopalswamy N, Michalek G, St Cyr O C, Plunkett S P, Rich N B & Howard R A, A catalog of white light coronal mass ejections observed by the SOHO spacecraft, *J Geophys Res (USA)*, 109 (2004) A07105.

4 Gopalswamy N, Energetic particle and other space weather events of solar cycle 24, *AIP Conf Proc (USA)*, 1500 (2012) pp 14-19.

5 Manoharan P K, Evolution of coronal mass ejections in the inner heliosphere: A study using white-light and scintillation images, *Sol Phys (Netherlands)*, 235 (2006) 345.

6 Chandra R, Gopalswamy N, Mäkelä P, Xie H, Yashiro S, Akiyama S, Uddin W, Srivastava A K, Joshi N C, Jain R, Awasthi A K, Manoharan P K, Mahalakshmi K, Dwivedi V C, Choudhary D P & Nitta N V, Solar energetic particle events during the rise phases of solar cycles 23 and 24, *Adv Space Res (UK)*, 52 (12) (2013) pp 2102-2111.

7 Yashiro S & Gopalswamy N, Statistical relationship between solar flares coronal mass ejections, In *Universal Heliophysical Processes: Proceedings of the International Astronomical Union* (Cambridge University Press, USA), 2008, 233.

8 Gopalswamy N, Yashiro S, Michalek G, Xie H, Mäkelä P, Vourlidas A & Howard R A, A catalog of halo coronal mass ejections from SOHO, *Sun Geosphere (The Republic of Azerbaijan)*, 5 (2010) 7.

9 Joshi N C, Uddin W, Srivastava A K, Chandra R, Gopalswamy N, Manoharan P K, Aschwanden M J, Choudhary D P, Jain R, Nitta N V, Xie H, Yashiro S, Akiyama S, Mäkelä P, Kayshap P, Awasthi A K, Dwivedi V C & Mahalakshmi K, A multi-wavelength study of eruptive events on January 23, 2012 associated with a major solar energetic particle event, *Adv Space Res (UK)*, 52 (1) (2013) pp 1-14.

10 Gopalswamy N, Yashiro S, Akiyama S, Mäkelä P, Xie H, Kaiser M L, Howard R A & Bougeret J L, Coronal mass ejections, type II radio bursts, and solar energetic particle events in the SOHO era, *Ann Geophys (Germany)*, 26 (10) (2008) pp 3033-3047.

11 Gopalswamy N, Xie H, Mäkelä P, Yashiro S, Akiyama S, Uddin W, Srivastava A K, Joshi N C, Chandra R, Manoharan P K, Mahalakshmi K, Dwivedi V C, Jain R, Awasthi A K, Nitta N V, Aschwanden M J & Choudhary D P, Height of shock formation in the solar corona inferred from observations of type II radio bursts and coronal mass ejections, *Adv Space Res (UK)*, 51 (11) (2013) pp 1981-1989.

12 Shanmugaraju A, Moon Y J & Vrsnak B, Type II Radio Bursts with high and low starting frequencies, *Sol Phys (Netherlands)*, 254 (2) (2009) pp 297-310.

13 Vrsnak B, Dynamics of solar coronal eruptions, *J Geophys Res (USA)*, 106 (A11) (2001) pp 25249-25259.

14 Anna Lakshmi M & Umapathy S, Coronal mass ejections associated with short and long duration X-ray flares, in International Symposium on Solar Terrestrial Physics, *Astron Soc India Conf Ser*, 10 (2013) pp 87-90.

15 Manoharan P K, Gopalswamy N, Yashiro S, Lara A, Michalek G & Howard R A, Influence of coronal mass ejection interaction on propagation of interplanetary shocks, *J Geophys Res (USA)*,109 (2004) A06109.

16 Gopalswamy N, Lara A, Kaiser M L & Bougeret J L, Near-Sun and near-Earth manifestations of solar eruptions, *J Geophys Res (USA)*, 106 (2001) pp 25261-25277.

17 Gopalswamy N, Aguilar-Rodriguez E, Yashiro S, Nunes S, Kaiser M L & Howard R A, Type II radio bursts and energetic solar eruptions, *J Geophys Res (USA)*, 110 (2005) A12S07.

18 Vrsnak B, Magdalenic J & Zlobec P, Band-splitting of coronal and interplanetary type II bursts – III: Physical conditions in the upper corona and interplanetary space, *Astron Astrophys (France)*, 413 (2004) pp 753-763.

19 Leblanc Y, Dulk G A & Bougeret J L, Tracing the electron density from the corona to 1 AU, *Sol Phys (Netherlands)*, 183 (1998) pp 165-180.

20 Pohjolainen S, Allawi H & Valtonen E, Origin of wide-band IP type II bursts, *Astron Astrophys (France),* 558 (2013) A7.

21 Srivastava Nandita & Venkatakrishnan P, Relationship between CME speed and geomagnetic storm intensity, *Geophys Res Lett (USA)*, 29 (9) (2002) 1287.